

# Two-stage Robust Nash Bargaining-based Benefit Sharing between Electric and HCNG Distribution Networks Bridged with SOFC

Wenwen Zhang, Gao Qiu, Hongjun Gao, *Member, IEEE*, Tingjian Liu, Junyong Liu, *Member, IEEE*, Yaping Li, Shengchun Yang, Jiahao Yan, Wenbo Mao

**Abstract**—Hydrogen-enriched compressed natural gas (HCNG) networks have potentized sustainability and efficiency of integrated electricity and natural gas systems (IENGs). However, paucity of benefit sharing risks the IENGs's development in multiple entities and bottlenecks its efficacy. To fill the gap, a robust Nash bargaining-based benefit sharing mechanism for HCNG-enabled IENGs is proposed. A cooperative scheduling model for HCNG and electric distribution network (EDN) bridged with solid oxide fuel cells (SOFCs) is firstly settled. In the sense, HCNG circumvents energy dissipation from hydrogen to methane, and SOFCs harvest efficient energy conversion from HCNG-to-power, so that to improve holistic welfare. To further stimulate the reciprocal coordination to actualize profits of the IENGs, a two-stage robust benefit sharing mechanism is proposed. In the first stage, Nash Bargaining model decides energy transaction volume and price. With aided robust dispatch of li-ion batteries, the second stage derisks the EDN's profit collapse from transaction bias, caused by forecasting errors of distributed renewable energy resources. Numerical studies indicate that, our framework reaps the decrease in energy conversion loss by 17%, 0.0412\$/kwh reduction on energy conversion cost, a stable social welfare of nearly 1.6% to total cost, and benefit-steady situations even in the worst case.

**Index Terms**—Hydrogen enriched compressed natural gas, two-stage robust, Nash bargaining, solid oxide fuel cells, hybrid energy storage system, li-ion battery

## NOMENCLATURE

### A. Abbreviation

HCNG	Hydrogen-enriched compressed natural gas
IENGs	Integrated electricity and natural gas systems
EDN	Electric distribution network
GDN	Gas distribution network
HGN	Higher-level gas network
P2G	Power to gas
G2P	Gas to power
DER	Distributed energy resource
ET	Electrolytic tank
HT	Hydrogen tank
SOFC	Solid oxide fuel cell
HESS	Hybrid energy storage system
C&CG	Column-and-constraint generation
ADMM	Alternating direction method of multipliers
BCD	Block coordinate descending

### B. Sets/Indices

$\mathbb{J}_1/\mathbb{J}_2/\mathbb{J}_3/\mathbb{J}_4$	Set of P2Gs/ G2Ps/li-ion batteries/DERs
$\mathbb{A}$	Set of nodes in GDN
$\mathbb{B}$	Set of nodes in EDN
$\mathbb{T}$	Set of operation periods

$m/n/g$	Index of natural gas nodes
$i/j/h$	Index of power nodes
$j_1/j_2/j_3/j_4$	Index of P2G/ G2P/ li-ion battery/ DER
$t$	Index of operation periods

### C. Parameters

$\Delta t$	Time interval
$\varepsilon_t$	Prices of natural gas
$\mu_t$	Prices of natural gas
$\vartheta_t^{P2G}$	Price of power for P2G
$\vartheta_t^{G2P}$	Price of gas for G2P
$\beta^{ET}/\beta^{SOFC}$	Power cost of ET/ SOFC
$\beta^{Li}/\alpha^{Li}$	Power/ capacity cost of li-ion battery
$\xi_{j_3}^{Li.min}/\xi_{j_3}^{Li.max}$	Minimum/maximum charge status
$w_m^{min}/w_m^{max}$	Minimum/ maximum node pressure
$\omega_{max}$	Max volume fraction of hydrogen
$\phi^{LD}/\phi^{DER}$	Volatility range of uncertainties
$c_{mn}$	Weymouth constant of the pipeline
$C^G/C^E$	Daily operating costs of GDN/EDN
$C^{HGN}$	Natural gas from HGN purchase costs
$C^{P2G}$	Purchase costs of gas from P2G
$C^{G2P}$	Purchase costs of electricity from G2P
$C^{TG}$	Purchase costs of electricity from upstream transmission grid
$C^{Li}/C^{SOFC}/C^{ET}$	Usage costs of li-ion battery/ SOFC/ET
$HHV^{CH_4}/HHV^{H_2}$	Higher heat value of CH <sub>4</sub> / H <sub>2</sub>
$P_{j_1}^{ET}/P_{j_2}^{SOFC}/P_{j_3}^{Li}$	Rated power of ET/SOFC/ li-ion battery
$E_{j_3}^{Li}$	Rated capacity of li-ion battery
$T^{ET}/T^{SOFC}/N_{j_3}^{Li}$	Lifetime of ET/SOFC/ li-ion battery
$U_i^{min}/U_i^{max}$	Min/max node voltage
$r_{ij}/x_{ij}$	Branch resistance/ reactance

### D. Variables

$P_{j_1,t}^{P2G}/P_{j_2,t}^{G2P}$	Power from P2G/G2P
$P_{j_3,t}^{Li}$	Li-ion battery charge power
$E_{j_3,t}^{Li}$	Li-ion battery store energy
$D_{j_3}$	Li-ion battery charge depth
$\xi_{j_3,t}^{Li}$	Li-ion battery charge status
$P_{j_4,t}^{DER}/Q_{j_4,t}^{DER}$	Active/reactive power injected by DER
$P_t^{TG}$	Electricity purchased from transmission

> REPLACE THIS LINE WITH YOUR MANUSCRIPT ID NUMBER (DOUBLE-CLICK HERE TO EDIT) <

	grid
$P_{j,t}^{LD}/Q_{j,t}^{LD}$	Active/ reactive power load
$I_{ij,t}$	Branch current
$U_{i,t}$	Node voltage
$P_{ij,t}/P_{jh,t}/$	Active power flow
$Q_{ij,t}/Q_{jh,t}$	Reactive power flow
$G_{j_2,t}^{G2P}$	Volume of gas from G2P
$G_{n,t}$	Equivalent gas load volume
$G_{mn,t}/G_{ng,t}$	Branch gas flow
$G_t^{HGN}$	Natural gas purchased from HGN
$G_{n,t}^{H_2}/G_{n,t}^{LD}$	Volume of hydrogen injection / gas load
$G_{j_1,t}^{HT}$	Hydrogen volume stored in HT
$w_{m,t}/w_{n,t}$	Node pressure
$HHV_t^{mix}$	Higher heat value of gas mixture
$G_t^{CH_4}/G_t^{H_2}$	CH4/ H2 injected into the pipeline
$\omega_t$	Volume fraction of hydrogen
$\eta^{P2G}/\eta^{P2G}$	Conversion efficiency of P2G/G2P
$P_{j,t}^{LD.pre}/P_{j_4,t}^{DER.pre}$	Power load/ DER output forecast value
$P_{j,t}^{LD.real}/P_{j_4,t}^{DER.real}$	Power load/ DER output actual value
$P_{j_3,t}^{Li.pre}$	Power of li-ion battery in the first stage
$\Delta P_{j_3,t}^{Li}$	Power adjustment value of li-ion battery in the second stage

## I. INTRODUCTION

To reduce dependence on fossil energy and also carbon emissions, distributed energy resources (DERs) are increasingly penetrating to EDN [1]- [2]. However, DER generation usually mismatch the load profiles due to its tremendous stochasticity, compromising DER utilization and stable EDN operation [3]. Recent research recognizes that, supported by late-model P2G and G2P technologies, natural gas network can actualize immense potential on consuming overflowing DER power via its linepack effect, whilst serve as controllable power sources to stabilize power grid [4]. IENGSSs have thus emerged as flexible way to manage uncertain DERs and promote energy efficacy, drawing growing studies worldwide [5].

To further unleash the flexibility and efficiency of IENGSS, several aspects capable of diminishing energy conversion loss have been noticed. From the perspective of improving the P2G path, the GDN enabling HCNG come out. It allows direct injection of hydrogen and hybrids of that and methane, such that conventional intermediate process of hydrogen-to-methane can be circumvented to save energy loss. [6] proposed a comprehensive HCNG operation model, upon which the performance of HCNG distribution networks is justified under various H<sub>2</sub> fractions and HCNG load portfolios. On the power grid side, SOFCs have been demonstrated the better electrical efficiency and the wider fuel adaptability against the common gas turbines [7], [8]. Existing literature also revealed that, oriented to power grid steady operation applications, SOFC can be generically modelled following the gas turbine's steady states [9]. Despite standalone investigations on either HCNG or SOFC are prevailing, way to unify their operations in a systematic IENGSS is still unprobed, such that the merits of HCNG-enabled IENGSS bridged with SOFCs are yet to be evaluated.

Upon the highly efficient infrastructure of HCNG-enabled GDN and SOFCs, profit pattern that advances development of the IENGSS becomes another imminent issue. Previous research has established that, centrally controlled IENGSS bespokes values in terms of stochasticity mitigation, renewable energy consumption, and social welfare increase [10]. More cognitions have manifested that centralized IENGSSs are away from engineering, where GDN and EDN are usually operated by different independent entities. Even though these entities partially privatize their information, [11] proved that IENGSS still benefits rich social welfare via the ADMM. In energy markets, in-depth problem for cooperative autonomous participants could come out, i.e., policy biases can render one stakeholder in weak position, and encumber the optimal social welfare [12]. Such policies can be, for example, economical penalties on renewable curtailment in power industries. Proper benefit sharing strategies are the key to solve the issue. The successes of Nash bargaining theory in other cooperative energy trading cases declare its salient merits on benefit sharing [13]- [14]. However, its availability in the IENGSS has not been investigated, let alone the concerned new IENGSS, where GDN dominates the cooperation due to efficient HCNG-fueled SOFC and HCNG network.

Despite benefit sharing can facilitate stable operation of IENGSS, profit collapse may still exist in the EDN side. Under the incentives of high-profit latency, SOFCs and HCNG network may participate more in EDN. Their slow responses force the EDN to buy costly electricity from upstream transmission grid to balance uncertainties of DERs [15], [16], triggering noticeable profit loss especially when there exists transactions bias due to over-prediction of DERs. [17] suggested configuring HESS to enhance rapid power balancing capability, and making look-ahead dispatch based on robust optimization to withstand slow-response hydrogen-to-power sources. Similar idea is also verified in [18], [19], where operational risks from uncertainties of renewable energy in traditional IENGSS are mitigated by two-stage robust model. But the foregoing studies were not embarked on more complicated benefit sharing for standalone GDN and EDN. [20] inspired to use BCD algorithm to ease the intact two-stage model into tractable tri-level equivalence. The BCD is however uncorroborated in mastering decentralized multi-entity IENGSS.

This paper brought forward configuration of multi-entity IENGSS, benefit sharing mechanism to promote win-win collaboration, and tailored algorithm to dispatch the whole system.

The main contributions are three-fold:

(1) A promising IENGSS model that bridges HCNG and electric distribution networks with SOFCs is proposed, where plethoric electricity produces hydrogen for HCNG, which is cyclically fed back to SOFCs to yield electricity. We show that such IENGSS can benefit in more potentiality of cooperative earnings across the two heterogenous entity networks. Specifically, HCNG avoids hydrogen to methane, reducing energy dissipation by 17%, and SOFCs save 0.0412\$/kwh of energy conversion cost versus gas turbines.

(2) Strong policy-directed economical penalties on renewable curtailment render the EDN precarious in transactions with the GDN, easily inducing abnormally negative pricing (or even failed pricing) for electrolytic hydrogen from P2G. This undesired circumstance can be exacerbated when HCNG network

> REPLACE THIS LINE WITH YOUR MANUSCRIPT ID NUMBER (DOUBLE-CLICK HERE TO EDIT) <

with higher energy conversion efficiency collaborates with EDN. To solve this issue, a Nash bargaining-based benefit sharing mechanism is firstly proposed for HCNG-enabled GDN and EDN bridged by SOFCs. It is designed upon ADMM to ensure basic privacy for both entities, and can promote an enduring and stable win-win situation to actualize the latent profits from efficient energy conversion.

(3) For the first time, a two-stage robust Nash bargaining strategy with binding batteries is proposed towards more economical and stable EDN. The first stage places the proposed Nash bargaining, and the second stage leverages robust dispatch of li-ion batteries to promote economic operation of the EDN. Besides, a new ADMM and BCD joint algorithm bridged by C&CG is proposed to efficiently resolve the complex two-stage model, where the second stage of robust battery dispatch is turned into a tractable tri-level form and promptly solved via BCD, and is looped with the Nash bargaining by C&CG.

## II. FRAMEWORK OF THE PROPOSED NCGN-ENABLED IENGs

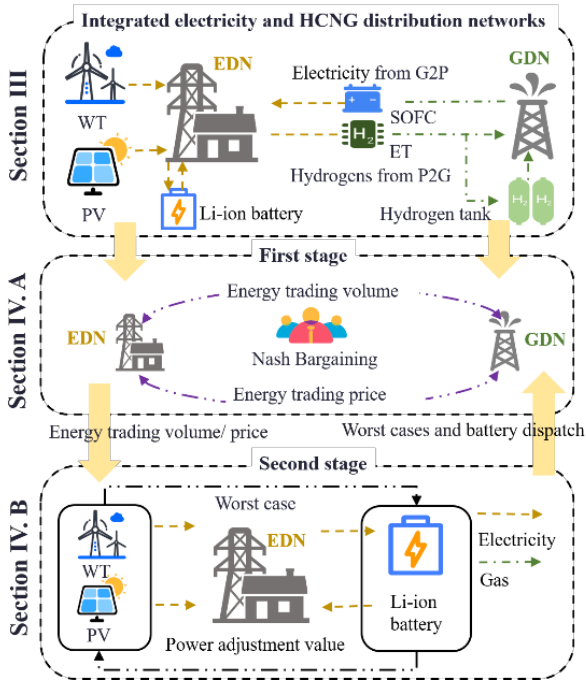


Fig. 1. The proposed two-stage robust benefit sharing framework.

Fig. 1 specifies the proposed two stage robust cooperative dispatch strategy for the two standalone entities of HCNG enabled GDN and EDN.

The first stage emulates the cooperative game between the two entities. Specifically, the transactions are carried out based on energy conversion infrastructures. The GDN is allowed to buy electricity from the EDN to yield hydrogen via ET, meanwhile the EDN can purchase HCNG from the GDN and generate power through HCNG-fueled SOFCs. To maximize social welfare and distribute benefits equally, Nash bargaining theory is adopted to settle the trading volume and prices in the designed transactions. The cooperative scheduling model and the benefit sharing strategy are depicted in section III and section IV. A, respectively.

The second stage takes in the trading volume as operational

baselines of energy conversion infrastructures, and conducts li-ion batteries to help the EDN alleviate the uncertainty by DERs. A designed subproblem is firstly employed to produce the worst operational cases under the given confidence intervals of DER power forecasts. Under these worst cases, dispatch for li-ion batteries is then settled to minimize purchasing electricity from upstream transmission grid and wipe out the transaction biases. After that, the li-ion battery dispatches and the produced worst cases are fed back to the first stage to correct the trading. The details of this stage are provided in section IV. B.

## III. SCHEDULING MODEL OF INTEGRATED ELECTRICITY AND HCNG DISTRIBUTION NETWORKS

Following the designated NCGN-enabled IENGs, we settle the cooperative scheduling model for both utilities of HCNG-enabled GDN (i.e., the HCNG network) and EDN. Each entity works to increase its own profit, and is allowed to interact with the other entity via P2G or G2P equipment for more benefits. To improve energy conversion efficiency and promote latent social welfare, we bring in highly efficient P2G facility of HCNG-enabled SOFC, and a compact HCNG network that can bypass additional conversion from hydrogen to methane.

### A. Scheduling Model of HCNG-enabled Network

The entity of the HCNG-enabled GDN intends to optimize its own yields, such that its own scheduling model will be set to maximize the income of selling gas to EDN, to minimize purchase cost of natural gas from HGN, purchase costs of hydrogen from P2G, and use costs of ET, and to adhere to operational constraints of HCNG network, as given below:

$$\begin{aligned} & \min_{P_{j_1,t}^{P2G}, G_{j_2,t}^{G2P}, G_{j_1,t}^{HT}, \vartheta_t^{P2G}, \vartheta_t^{G2P}} C^G \quad (1) \\ & \begin{cases} C^G = C^{HGN} + C^{P2G} + C^{ET} - C^{G2P} \\ C^{HGN} = \sum_t \varepsilon_t G_t^{HGN} \\ C^{P2G} = \sum_j \sum_t \vartheta_t^{P2G} P_{j_1,t}^{P2G} \\ C^{ET} = \sum_{j_1} \sum_t \frac{\beta^{ET} P_{j_1,t}^{P2G} \Delta t}{P_{j_1}^{ET} T^{ET}} \\ C^{G2P} = \sum_{j_2} \sum_t \vartheta_t^{G2P} G_{j_2,t}^{G2P} \end{cases} \quad (2) \end{aligned}$$

$$G_{n,t} = \sum_m G_{mn,t} + G_{n,t}^{H_2} + G_{n,t}^{HGN} - \sum_g G_{ng,t} + G_{n,t}^{G2P} \quad (3)$$

$$G_{j_1,t}^{H_2} = \frac{\eta^{P2G} \cdot P_{j_1,t}^{P2G} \Delta t}{HHV^{H_2}} - G_{j_1,t}^{HT} \quad (4)$$

$$G_{n,t} = (G_{n,t}^{LOAD} \cdot HHV^{CH_4}) / HHV_t^{mix} \quad (5)$$

$$\omega_t = G_t^{H_2} / (G_t^{H_2} + G_t^{CH_4}), \quad \omega_t \leq \omega_{max} \quad (6)$$

$$HHV_t^{mix} = \omega_t HHV^{H_2} + (1 - \omega_t) HHV^{CH_4} \quad (7)$$

$$G_{mn,t} = \tau_{mn,t} \cdot c_{mn} \sqrt{\tau_{mn,t} (w_{m,t}^2 - w_{n,t}^2)} \quad (8)$$

$$\tau_{mn,t} = \begin{cases} 1 & w_{m,t} \geq w_{n,t} \\ -1 & w_{m,t} \leq w_{n,t} \end{cases} \quad (9)$$

$$\left\| \frac{G_{mn,t}}{c_{mn} w_{n,t}} \right\|_2 \leq c_{mn} w_{m,t}, \quad w_{m,t}^{min} \leq w_{m,t} \leq w_{m,t}^{max} \quad (10)$$

$$\begin{aligned} & \min_{P_{j_1,t}^{P2G}, G_{j_2,t}^{G2P}, G_{j_1,t}^{HT}, \vartheta_t^{P2G}, \vartheta_t^{G2P}} (C^G + \sum_t \sum_{m,n} \tau(w_{m,t} - w_{n,t})) \quad (11) \\ & \forall t \in \mathbb{T}, j_1 \in \mathbb{J}_1, j_2 \in \mathbb{J}_2, m/n/g \in \mathbb{A} \end{aligned}$$

where the balance constraints of the gas network nodes are presented as (3)-(4). Changes in gas composition can affect the consumed volume [21], equivalent replacement of gas loads as

> REPLACE THIS LINE WITH YOUR MANUSCRIPT ID NUMBER (DOUBLE-CLICK HERE TO EDIT) <

shown in (5)-(7). The steady-state natural gas power flow constraints are formulated as (8)-(9) upon Weymouth equation. Considering that the GDN is radiant, the second-order cone relaxation can be used to convexify the constraints (8)-(9) into (10) [22]. To ensure that the second-order cone relaxation of natural gas power flow is exact, a penalty term on the nodal pressure difference is added to the objective function [23].

### B. Scheduling Model of Electric Distribution Network

The optimization goal of the EDN is to minimize daily operating costs in the worst scenarios, including purchase costs of electricity from upstream transmission grid, purchase costs of electricity from G2P units, and HESS usage costs, and to maximize incomes from the sale of P2G gas, as shown in (12)-(13).

$$\begin{aligned} & \min_{P_{j_3,t}^{Li}, P_{j_1,t}^{P2G}, P_{j_2,t}^{G2P}, \theta_t^{P2G}, \theta_t^{G2P}} C^E \quad (12) \\ & \begin{cases} C^E = C^{G2P} + C^{TG} + C^{HESS} - C^{P2G} \\ C^{TG} = \sum_t \mu_t P_t^{TG} \\ C^{HESS} = C^{Li} + C^{SOFC} \\ C^{Li} = \sum_{j_3} \frac{\sum_{t=1}^T ((\alpha^{Li} E_{j_3}^{Li} + \beta^{Li} P_{j_3}^{Li}) \cdot |P_{j_3,t}^{Li}| \cdot \Delta t)}{N_{j_3}^{Li} \cdot E_{j_3}^{Li} \cdot D_{j_3}} \\ N_{j_3}^{Li} = 28270e^{(-2.401D_{j_3})} + 2.214e^{(5.901D_{j_3})} \\ C^{SOFC} = \sum_{j_2} \sum_t \frac{\beta^{SOFC} P_{j_2,t}^{G2P} \Delta t}{P_{j_2}^{SOFC} T^{SOFC}} \end{cases} \quad (13) \\ & \forall t \in \mathbb{T}, j_2 \in \mathbb{J}_2, j_3 \in \mathbb{J}_3 \end{aligned}$$

where HESS usage costs consist of li-ion battery usage costs  $C^{Li}$  and SOFC usage costs  $C^{SOFC}$ .  $C^{Li}$  considers that depth of discharge (DOD) can affect the cycle life of li-ion battery [24],  $N_{j_3}^{Li}$  is the number of cycles when the DOD is  $D_{j_3}$ .

Distribution network power flow is formed as a standard second-order cone as in (14)-(15). (16)-(20) show the voltage security and power balance constraints for each bus in EDN. (21)-(23) are the operational constraints of li-ion batteries, SOFCs, ETs, respectively, and they are the constraints built upon random variables.

$$\hat{I}_{ij,t} = I_{ij,t}^2, \hat{U}_{i,t} = U_{i,t}^2 \quad (14)$$

$$\left\| \begin{array}{l} 2P_{ij,t} \\ 2Q_{ij,t} \end{array} \right\| \leq \hat{I}_{ij,t} + \hat{U}_{i,t} \quad (15)$$

$$(U_i^{min})^2 \leq \hat{U}_{i,t} \leq (U_i^{max})^2 \quad (16)$$

$$P_{j,t}^{LOAD} = \sum_i P_{ij,t} - r_{ij} \hat{I}_{ij,t} - \sum_h P_{jh,t} + P_{j,t}^{DER} + P_{j,t}^{G2P} + P_{j,t}^{Li} - P_{j,t}^{P2G} \quad (17)$$

$$P_{j_2,t}^{G2P} = G_{j_2,t}^{G2P} \cdot HHV_t^{mix} \quad (18)$$

$$P_{j_3,t}^{Li} = P_{j_3,t}^{Li,pre} \quad (19)$$

$$Q_{j,t}^{LOAD} = \sum_i Q_{ij,t} - x_{ij} \hat{I}_{ij,t} - \sum_h Q_{jh,t} + Q_{j,t}^{DER} \quad (20)$$

$$E_{j_3,t}^{Li} = E_{j_3,t-1}^{Li} + \int_{t-1}^t P_{j_3,t}^{Li} \quad (21)$$

$$\xi_{j_3,t}^{Li} = E_{j_3,t}^{Li} / E_{j_3}^{Li}, \xi_{j_3,t}^{Li, min} \leq \xi_{j_3,t}^{Li} \leq \xi_{j_3,t}^{Li, max} \quad (22)$$

$$\begin{cases} -P_{j_3}^{Li} \leq P_{j_3,t}^{Li} \leq P_{j_3}^{Li} \\ 0 \leq P_{j_2,t}^{G2P} \leq P_{j_2}^{SOFC}, 0 \leq P_{j_1,t}^{P2G} \leq P_{j_1}^{ET} \end{cases} \quad (23)$$

$$\forall t \in \mathbb{T}, j_1 \in \mathbb{J}_1, j_2 \in \mathbb{J}_2, j_3 \in \mathbb{J}_3, i, j, h \in \mathbb{B}$$

## IV. TWO-STAGE ROBUST NASH BARGAINING-BASED BENEFIT SHARING BETWEEN HCNG NETWORK AND EDN

To actualize the social welfare of the IENGs set on the HCNG network and the EDN, an all-win cooperation is imperative. Otherwise, EDN will be placed in a weak position, since it is stressed to consume RES, but HCNG network features requisite energy storage property to this end. To guarantee the benefits for the participating utilities, this section firstly introduces a privacy-preserving benefit sharing mechanism based on Nash bargaining theory and ADMM. On the other hand, motivated by the salient energy conversion efficiency of SOFCs and HCNG network, their foreseeable aggressive participation can jeopardize the EDN's ability to follow the shift of DER. Whereon, to de-risk reciprocity dis-equilibration between the two entities, a robust scheduling aided by li-ion batteries will be drawn into the whole cooperative model. Packed the above built models together via C&CG, we finally settle a two-stage robust Nash bargaining model aimed at stable social welfare. Coordination of interdependent natural gas and electricity infrastructures for firming the variability of wind energy in stochastic day ahead scheduling

### A. Nash Bargaining between HCNG Network and EDN

The interaction between the GDN and the EDN is modelled using cooperative game, and the Pareto optimum between the two entities can be achieved fairly by constructing the following Nash bargaining model:

$$\begin{cases} \max_{P_{j_1,t}^{P2G}, P_{j_2,t}^{G2P}, \theta_t^{P2G}, \theta_t^{G2P}} (C_0^E - C^E)(C_0^G - C^G) \\ C^E \leq C_0^E, C^G \leq C_0^G \\ \text{s. t. (2)-(11), (13)-(23), } \forall t \in \mathbb{T}, j_1 \in \mathbb{J}_1, j_2 \in \mathbb{J}_2 \end{cases} \quad (24)$$

where  $C_0^E, C_0^G$  are the operating costs of EDN and GDN when they operate independently.

To solve the problem (24), we equivalently transform (24) into total benefit maximization problem (**Question 1**). The transaction price variables ( $[\theta_t^{P2G}, \theta_t^{G2P}]$ ) in **Question 1** are eliminated, thus the volume of energy transaction ( $[P_{j_1,t}^{P2G}, G_{j_2,t}^{G2P}]$ ) in **Question 1** can be directly solved to obtain the solution  $[\check{P}_{j_1,t}^{P2G}, \check{G}_{j_2,t}^{G2P}]$ .

#### Question 1:

$$\begin{cases} \max_{P_{j_1,t}^{P2G}, P_{j_2,t}^{G2P}} (C_0^E - C^{NET} - C^{HESS}) + (C_0^G - C^{HGN} - C^{ET}) \\ C^{NET} + C^{HESS} \leq C_0^E, C^{HGN} - C^{ET} \leq C_0^G \\ \text{s. t. (2)-(11), (13)-(23), } \forall t \in \mathbb{T}, j_1 \in \mathbb{J}_1, j_2 \in \mathbb{J}_2 \end{cases} \quad (25)$$

By converting (24) into logarithmic form, we obtain another equivalent optimization problem (**Question 2**).

#### Question 2:

$$\begin{cases} \max_{\theta_t^{P2G}, \theta_t^{G2P}} \ln(C_0^E - C^E) + \ln(C_0^G - C^G) \\ C^E \leq C_0^E, C^G \leq C_0^G \\ \text{s. t. (2)-(11), (13)-(23), } \forall t \in \mathbb{T} \end{cases} \quad (26)$$

where decision variables  $[P_{j_1,t}^{P2G}, G_{j_2,t}^{G2P}]$  are replaced with fixed parameter  $[\check{P}_{j_1,t}^{P2G}, \check{G}_{j_2,t}^{G2P}]$ . Whereupon optimal energy transaction prices  $[\check{\theta}_t^{P2G}, \check{\theta}_t^{G2P}]$  can be obtained by solving (26).

To ensure the privacy of the internal information of each entity, distributed optimization formulation (28)-(31) of (25)-(26) are built based on ADMM algorithm. Besides, to decouple

> REPLACE THIS LINE WITH YOUR MANUSCRIPT ID NUMBER (DOUBLE-CLICK HERE TO EDIT) <

$[P_{j_1,t}^{P2G}, G_{j_2,t}^{G2P}]$  and  $[\vartheta_t^{P2G}, \vartheta_t^{G2P}]$ , auxiliary variables are introduced in constraint (27) which needs to be enforced in the later.

$$\begin{cases} P_{j_1,t}^{P2GG} = P_{j_1,t}^{P2GP}, G_{j_2,t}^{G2PG} = G_{j_2,t}^{G2PP} \\ \vartheta_t^{P2GG} = \vartheta_t^{P2GP}, \vartheta_t^{G2PG} = \vartheta_t^{G2PP} \\ \forall t \in \mathbb{T}, j_1 \in \mathbb{J}_1, j_2 \in \mathbb{J}_2 \end{cases} \quad (27)$$

where  $[P_{j_1,t}^{P2GG}, G_{j_2,t}^{G2PG}, \vartheta_t^{P2GG}, \vartheta_t^{G2PG}]$  represents the GDN's willingness to trade,  $[P_{j_1,t}^{P2GP}, G_{j_2,t}^{G2PP}, \vartheta_t^{P2GP}, \vartheta_t^{G2PP}]$  represents the EDN's willingness to trade.

### Question 1:

$$\begin{cases} \min L_1^E = C^{NET} + C^{HESS} - C_0^E + \\ \sum_{j_1} \sum_t \chi_{j_1,t}^P (P_{j_1,t}^{P2GG} - P_{j_1,t}^{P2GP}) + \frac{\rho_1}{2} (P_{j_1,t}^{P2GG} - P_{j_1,t}^{P2GP})^2 + \\ \sum_{j_2} \sum_t \chi_{j_2,t}^G (G_{j_2,t}^{G2PG} - G_{j_2,t}^{G2PP}) + \frac{\rho_2}{2} (G_{j_2,t}^{G2PG} - G_{j_2,t}^{G2PP})^2 \\ \text{s. t. (13)-(23), } \forall t \in \mathbb{T}, j_1 \in \mathbb{J}_1, j_2 \in \mathbb{J}_2 \end{cases} \quad (28)$$

$$\begin{cases} \min L_1^G = C^{GR} + C^{ET} - C_0^G + \\ \sum_{j_1} \sum_t \chi_{j_1,t}^P (P_{j_1,t}^{P2GG} - P_{j_1,t}^{P2GP}) + \frac{\rho_1}{2} (P_{j_1,t}^{P2GG} - P_{j_1,t}^{P2GP})^2 + \\ \sum_{j_2} \sum_t \chi_{j_2,t}^G (G_{j_2,t}^{G2PG} - G_{j_2,t}^{G2PP}) + \frac{\rho_2}{2} (G_{j_2,t}^{G2PG} - G_{j_2,t}^{G2PP})^2 \\ \text{s. t. (2)-(11), } \forall t \in \mathbb{T}, j_1 \in \mathbb{J}_1, j_2 \in \mathbb{J}_2 \end{cases} \quad (29)$$

### Question 2:

$$\begin{cases} \min L_2^E = -\ln(C_0^E - C^E) + \\ \sum_t \gamma_t^P (\vartheta_t^{P2GG} - \vartheta_t^{P2GP}) + \frac{\rho_3}{2} (\vartheta_t^{P2GG} - \vartheta_t^{P2GP})^2 + \\ \sum_t \gamma_t^G (\vartheta_t^{G2PG} - \vartheta_t^{G2PP}) + \frac{\rho_4}{2} (\vartheta_t^{G2PG} - \vartheta_t^{G2PP})^2 \\ \text{s. t. (13)-(23), } \forall t \in \mathbb{T} \end{cases} \quad (30)$$

$$\begin{cases} \min L_2^G = -\ln(C_0^G - C^G) + \\ \sum_t \gamma_t^P (\vartheta_t^{P2GG} - \vartheta_t^{P2GP}) + \frac{\rho_3}{2} (\vartheta_t^{P2GG} - \vartheta_t^{P2GP})^2 + \\ \sum_t \gamma_t^G (\vartheta_t^{G2PG} - \vartheta_t^{G2PP}) + \frac{\rho_4}{2} (\vartheta_t^{G2PG} - \vartheta_t^{G2PP})^2 \\ \text{s. t. (2)-(11), } \forall t \in \mathbb{T} \end{cases} \quad (31)$$

where  $L_1^E, L_1^G$  ( $L_2^E, L_2^G$ ) are the augmented Lagrangian functions for the EDN and GDN about **Question 1** (**Question 2**).  $\chi_{j_1,t}^P, \chi_{j_2,t}^G, \gamma_t^P, \gamma_t^G, \rho_1, \rho_2, \rho_3, \rho_4$  are the Lagrangian multipliers.

## B. Two-stage Robust Nash Bargaining Involving Li-ion Battery and Its Solving Scheme

Taking account of uncertainties, the EDN is at risk of failing to achieve the desired effect of prior trading decisions, therefore, a two-stage robust model is established, as shown in (32)-(33).

$$\min_y \max_u \min_x C^E \quad (32)$$

$$\begin{cases} \text{s. t. (13)-(23)} \\ P_{j_3,t}^{Li} = P_{j_3,t}^{Li.pre} + \Delta P_{j_3,t}^{Li} \\ 0 \leq (P_{j_4,t}^{LOAD.real} - P_{j_4,t}^{LOAD.pre}) / P_{j_4,t}^{LOAD.pre} \leq \phi^{LOAD} \\ 0 \leq (P_{j_4,t}^{DER.real} - P_{j_4,t}^{DER.pre}) / P_{j_4,t}^{DER.pre} \leq \phi^{DER} \\ 0 \leq P_{j_4,t}^{DER} \leq P_{j_4,t}^{DER.real}, P_{j_4,t}^{LOAD} = P_{j_4,t}^{LOAD.real} \\ \forall t \in \mathbb{T}, j_1 \in \mathbb{J}_1, j_2 \in \mathbb{J}_2, j_3 \in \mathbb{J}_3, j_4 \in \mathbb{J}_4, j \in \mathbb{B} \end{cases} \quad (33)$$

where  $\mathbf{y} = [P_{j_3,t}^{Li.pre}, P_{j_1,t}^{P2G}, P_{j_2,t}^{G2P}, \vartheta_t^{P2G}, \vartheta_t^{G2P}]$  is the first stage decision variable,  $\mathbf{x} = [\Delta P_{j_3,t}^{Li}]$ , is the second stage decision variable,  $\mathbf{u} = [P_{j_4,t}^{LOAD.real}, P_{j_4,t}^{DER.real}]$ . is the worst case of uncertain variable. Besides, based on constraints (13)-(23), the constraints of uncertain variables are added to constraint (33).

Through C&CG algorithm, the two-stage robust model is

decomposed into the main problem (MP) and the subproblem (SP). As shown in Fig. 2, the MP serves to optimize the volume and prices of the energy transaction, through the model presented in section IV. A. The sub-problem is responsible for figuring out the worst cases of random variables, and planning the power adjustment profiles of li-ion batteries to de-risk profit collapse due to stochastic nature of DERs.

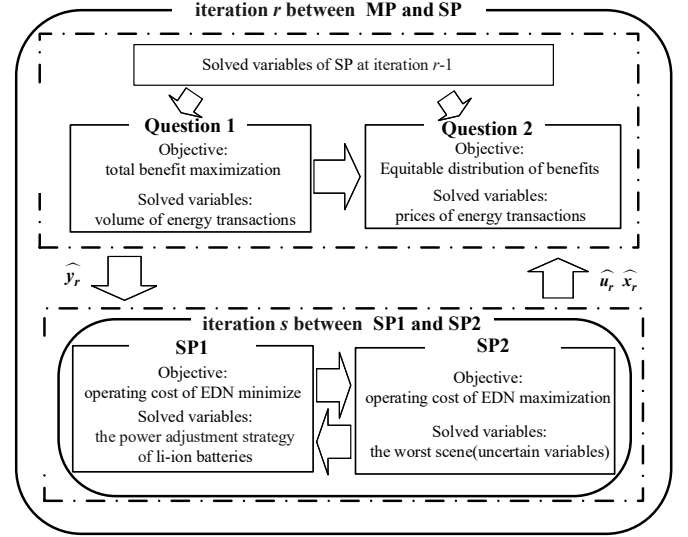


**Fig. 2.** Solving scheme of the proposed two-stage robust benefit sharing model between HCNG-enabled GDN and EDN

The MP and SP at iteration  $r$  of the C&CG algorithm is formulated as (34)-(35).

$$\text{MP: } \begin{cases} (28)-(31) \\ \mathbf{x} = \hat{\mathbf{x}}_{r-1}, \mathbf{u} = \hat{\mathbf{u}}_{r-1} \end{cases} \quad (34)$$

$$\text{SP: } \begin{cases} \max_{\mathbf{x}} \min_{\mathbf{u}} C^E \\ \mathbf{y} = \hat{\mathbf{y}}_r \\ \text{s. t. (13)-(23)} \end{cases} \quad (35)$$

where  $\hat{\mathbf{x}}_{r-1}, \hat{\mathbf{u}}_{r-1}$  are solutions of decision variable in the second stage and the worst case of SP, respectively, at iteration  $r-1$ , which will be set to a cutting plane constraints of MP.  $\hat{\mathbf{y}}_r$  is decision variable of MP solved in the first stage, at iteration  $r$ , which will be set to cutting plane constraints of MP. In this regard, MP and SP become a two-level solving loop.

Since the SP is a max-min problem and cannot be solved directly, to solve it, the BCD algorithm is used to decompose the SP into two tractable problems of subproblem1 (SP1) and subproblem2 (SP2). Note that, SP1 and SP2 construct an inner loop of their upstream solving loop of MP-SP.

In the at sth iteration of SP1-SP2 inner solving loop, the BCD algorithm sequentially solves (36) and (37).

$$\text{SP1: } \begin{cases} C_{r,s}^{E,SP} = \min_{\mathbf{x}} C^E \\ \mathbf{y} = \hat{\mathbf{y}}_r, \mathbf{u} = \hat{\mathbf{u}}_{r,s-1} \\ \text{s. t. (13)-(23)} \end{cases} \quad (36)$$

where the random variables  $\mathbf{u}$  are fixed as  $\hat{\mathbf{u}}_{r,s-1}$ , which is the worst case of SP2 at iteration  $s-1$ , during the  $r$ th solving loop of MP and SP.



> REPLACE THIS LINE WITH YOUR MANUSCRIPT ID NUMBER (DOUBLE-CLICK HERE TO EDIT) <

$$\text{SP2: } \begin{cases} \max_{\mathbf{u}} \check{C}_{r,s}^{E,SP} + \sum_j \sum_t a_{j,t} (P_{j,t}^{LD,real} - \check{P}_{j,t}^{LD,real,r,s-1}) \\ \quad + \sum_{j_4} \sum_t e_{j_4,t} (P_{j_4,t}^{DER,real} - \check{P}_{j_4,t}^{DER,real,r,s-1}) \\ \mathbf{y} = \check{\mathbf{y}}_r, \mathbf{x} = \check{\mathbf{x}}_{r,s} \\ \text{s.t. (13)-(23), } \forall t \in \mathbb{T}, j_4 \in \mathbb{J}_4, j \in \mathbb{B} \end{cases} \quad (37)$$

SP2 is the first order Taylor expansion of SP1 at  $\mathbf{u}$ .  $\check{C}_{r,s}^{E,SP}$  is the objective solution of SP1 at iteration  $s$ ,  $a_{j,t}$  and  $e_{j_4,t}$  are the sensitivities of  $C_r^E$  at  $\check{\mathbf{u}}_{r,s-1} = [\check{P}_{j,t}^{LD,real,r,s-1}, \check{P}_{j_4,t}^{DER,real,r,s-1}]$ . In this solving process,  $\mathbf{x}$  is fixed as  $\check{\mathbf{x}}_{r,s}$ , which is the optimal decision variable of SP1 at iteration  $s$ .

## V. NUMERICAL STUDIES

A IENGs consisting of an IEEE 33-bus EDN and a 20-node Belgian GDN is studied, as shown in Fig.3, where solar and wind power generation data are from Elia, power and gas load data are collected from [25]. In IEEE 33-bus EDN, DERs are integrated at bus E17, E21, E24, and E32, bus E17 and E32 own li-ion batteries, bus E6 and E12 are connected to node G8 and G4 of the GDN through SOFCs. Voltage limits of all power buses are within [0.95, 1.05] p.u. The uncertainties of DER generation and load are simulated via 15% and 5% intervals upon their forecasting baselines. In 20-node GDN, HT is integrated at node G0, and two ETs are set on node E17 and E24.

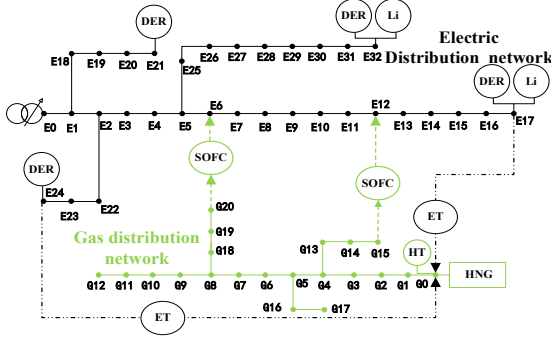


Fig. 3. Configuration diagram of combined optimization model between electricity and HCNG distribution networks.

### A. Efficiency analysis of cooperative EDN and GDN

To prove the effectiveness of the proposed cooperative operational framework, three competitive models are given:

**Model 1:** The proposed cooperative EDN and GDN.

**Model 2:** No cooperation between EDN and GDN. Following [26], EDN configures its own li-ion batteries, HT and SOFCs, and goes self-energy conversion between electricity and hydrogen. The **Model 2** can be deemed as a development of the architecture in [27], and it can help figure out if SOFCs can turn this self-energy conversion loop to be profitable.

**Model 3:** No cooperation between EDN and GDN, and only li-ion batteries are included in EDN [28]. This is a common case known as active distribution network. The **Model 3** come out to highlight the high capacity and cost-effectiveness merits of the proposed IENGs architecture.

Without uncertainty involved, the daily operating costs, energy conversion loss rate, and the marginal cost of ET and SOFC (i.e., the sensitivity of their cost versus the produced

energy) are shown in Tab. I. Benefit ingredients and energy conversion profiles are shown in Tab. II and Fig. 4, respectively.

TABLE I  
DAILY OPERATING COSTS WITHOUT UNCERTAINTY CONSIDERED

Model #	Operating Costs \$	Energy Conversion Loss Rate	Marginal cost \$/kWh
<b>Model 1</b>	EDN <b>1537</b>	<b>27%</b>	<b>0.0307</b>
	GDN <b>23614</b>		
<b>Model 2</b>	EDN 1699	44%	0.0719
	GDN 23809		
<b>Model 3</b>	EDN 1755	-	-
	GDN 23809		

TABLE II  
INGREDIENTS ANALYSIS OF COST AND BENEFIT (\$)

Model	Benefit*	$C^{SOFC}$	$C^{ET}$	$C^{TG}$	$C^{HGN}$
<b>Model 1</b>	EDN 218	273	116	240	24220
	GDN 194				
<b>Model 2</b>	EDN 56	27	34	1271	23809

\*Benefits of EDN and GDN are calculated via  $C_0^E - C^E$  and  $C_0^G - C^G$ , respectively.

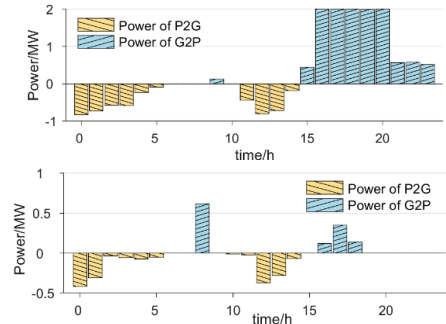


Fig. 4. Energy conversion profiles. Note that, positive power indicates that the energy conversion runs from gas to power, also the power injection to the EDN (top: **Model 1**. bottom: **Model 2**).

From Tab. I and Tab. II, daily operating cost of EDN by **Model 1** is similar to that by **Model 2**, both reducing the EDN's cost by nearly 12% against **Model 3**. However, **Model 1** significantly outperform **Model 2** regarding daily operating costs of GDN. **Model 1** creates the best social welfare which is nearly 1.6% to total cost, while guaranteeing EDN benefits. In **Model 1**, the EDN gets profits by either selling hydrogen or buying HCNG to generate electricity below the time-of-use electricity price, and GDN earns by two paths of selling natural gas and yielding low-priced hydrogen. Whereas, in **Model 2**, EDN can only gain from the price gap between the low-priced local renewable energies and the high-priced electricity of upstream grid. Besides, **Model 2** only allows conversion between pure hydrogen and power, without off-the-shelf fuel supplement from GDN, it thus results in an enormous energy loss rate of 44%, and is beat by **Model 1** in term of energy conversion's marginal cost (i.e., 0.0719 \$/kWh vs. 0.0307 \$/kWh), which implies the waste of energy and the decline in social welfares.

In addition, from Fig. 4, **Model 1** successfully distributes the yielded benefits to EDN and GDN through the Nash bargaining model This demonstrates the feasibility of the proposed benefit sharing strategy.

### B. Verification of the proposed robust benefit sharing strategy

Robust benefit sharing de-risks profit collapse due to

> REPLACE THIS LINE WITH YOUR MANUSCRIPT ID NUMBER (DOUBLE-CLICK HERE TO EDIT) <

forecasting error. Here we consider three robust cases (**Case 2~Case 4**). Notably, **Case 1** is a deterministic case that assumes forecasts are exact, which in fact corresponds to single MP.

**Case 1:** The forecasts of load and DERs generation are exact.

**Case 2:** The forecast of DER generation is exact, while load profile is produced by the robust optimization procedure SP2.

**Case 3:** The forecast of load is exact, DER generation profile is produced by the robust optimization procedure SP2.

**Case 4:** Load and DERs generation profiles are both produced by the robust optimization procedure SP2.

**Case 2~Case 4** establish the testing robust operational set. To show the importance of li-ion batteries in robust benefit sharing, daily operating costs with or without lithium battery power redispatch as shown in Tab. III.

TABLE III

OPERATING COSTS WITH OR WITHOUT LI-ION BATTERY POWER REDISPATCH (\$)

Entities	Case 1	Case 2		Case 3		Case 4	
		No bat.	With bat.	No bat.	With bat.	No bat.	With bat.
EDN	1537	2017	1922	3038	2859	3636	3459
GDN	23614	23614		23614		23614	

From Tab. III, two results can be found. The one is a trivial conclusion, which indicates that operating costs increase along with consideration of robustness. On the other hand, under **Case 2~Case 4**, li-ion batteries help improve operational economic by nearly 5.5% on average. The reason is that, the slow responses of SOFCs and ETs cannot balance the power drift of stochastic variables (DER generation and load) in real-time, so the EDN can only conduct either fast power regulation equipment or buy electricity from upstream transmission grid towards power balance. By li-ion batteries, the costly electricity purchase from transmission grid can be reduced, even though lifetime operational costs are embraced in dispatch.

We further study how the robust benefit sharing help mitigate profit collapse for the EDN, and Tab. IV is whereupon provided below. Since forecasting error of load and DER generation exists, there must be power imbalances in intraday operations. Towards power balance, whether the EDN pays auxiliary service fees to li-ion batteries or purchases electricity from upstream transmission grid, its profit collapse always comes from the transaction bias between the day-ahead cooperative IENGs schedule and intraday true operations of load and DERs. So, a trivial assumption that only considers electricity purchase from upstream power grid is made during the forming of Tab. IV.

TABLE IV

IMPLEMENTATION COSTS OF DAY-AHEAD SCHEDULES ON INTRADAY CASES (\$)

Testing intraday operational case/set	Proposed Robust benefit sharing (with SP)		Deterministic benefit sharing (excluding SP)	
	$C^E$	$C^{TG}$	$C^E$	$C^{TG}$
<b>Case 1</b>	1537	240	1537	240
<b>Case 2</b>	1906	399	1922	857
<b>Case 3</b>	2551	776	2859	1919
<b>Case 4</b>	3089	1250	3459	2519
<i>Mean±var. stat. under robust set</i>	2271±595	666±389	2444±758	1309±892

In Tab. IV, there is clear trends of decreasing operating cost

of the EDN ( $C^E$ ) by the proposed method. Also, more uncertainties enlarge the risk of profit collapse, as you can see **Case 4** manifests the largest increase of cost in the comparison between our method and the deterministic one. The cost statistics revealed that, the robust strategy indeed stabilizes the profit of the EDN to withstand forecasting errors of uncertainties, and its decision pattern is to facilitate interactions between the EDN and the GDN to reduce costly electricity purchase from upstream power grid ( $C^{TG}$ ), which will be further analyzed later.

To further justify the proposed framework, Tab. V, Fig. 5, Fig. 6, and Fig. 7 are provided. These outcomes stem from comparative experiments under the given robust operating cases.

TABLE V

TOTAL OPERATING COSTS BY COMPETITIVE MODELS IN DIFFERENT ROBUST CASES (\$)

Case #	Entities	Model 1	Model 2	Model 3
<b>Case 2</b>	EDN	1906	2011	2143
	GDN	23579	23809	23809
<b>Case 3</b>	EDN	2551	2816	2820
	GDN	23558	23809	23809
<b>Case 4</b>	EDN	3089	3382	3382
	GDN	23480	23809	23809

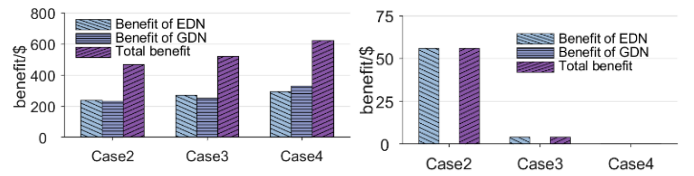


Fig. 5. Benefit analysis (left: **Model 1**. right: **Model 2**).

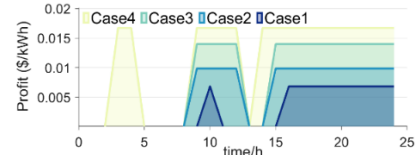


Fig. 6. Marginal profit of the GDN selling HCNG upon the proposed benefit sharing mechanism (**Model 1**) under the testing robust cases.

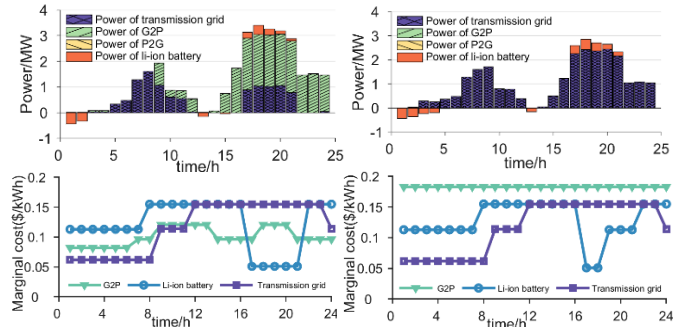


Fig. 7. Profiles of operations and marginal costs of involved infrastructures under **Case 4** (left column: **Model 1**. Right column: **Model 2**).

Tab. V and Fig. 5 present the best cost-benefit stability of the proposed method compared to other rivals. Illustrative data are the dramatically decreasing benefit by **Model 2** from **Case 2** to **Case 3**, as shown in the bottom subplot of Fig. 5. Relatively, our method gains stable benefits for both EDN and GDN, no matter what extreme cases happen. Besides, it is apparent that, **Model 1** results in the best economy of GDN, as GDN can gain extra benefits by energy conversion with EDN. We can further explain the above conditions by means of Fig. 6. In Fig. 6, marginal profit of the GDN selling HCNG increases from **Case 1**

> REPLACE THIS LINE WITH YOUR MANUSCRIPT ID NUMBER (DOUBLE-CLICK HERE TO EDIT) <

to the worst **Case 4**. The worse operating cases of the EDN incent more sale of HCNG fuel from the GDN, such that the GDN earns more. The incomes will then be shared to the EDN to contribute to a risk-averse and stable benefits for both entities. In this win-win situation, GDN gains extra payback and help stabilize the operation of EDN to consolidate ongoing gains. Yet, this is not the case for **Model 2**, since in contrast to the tremendous gas storage of the GDN, the storage capacity of self-hydrogen and electricity conversion is negligible and of high use expense, hydrogen storage cannot be benefited.

Fig. 7 interprets the significance of the SOFC-bridged cooperative mechanism between the EDN and the HCNG-enabled GDN. As shown in Fig. 7, during 15~24 h where DER generation plummet, G2P transactions in the framework of **Model 1** are prolifically stimulated, because of two origins. On one hand, upon our designed IENGs, marginal cost of HCNG-to-power is stable and regulated much lower than that of electricity from upstream grid. On the other hand, although li-ion batteries hold the best marginal cost, they lack controllable capacity to serve as critical flexible resources in such extreme **Case 4**, whereas GDN's storage capacity is immense. Regarding **Model 2**, self-hydrogen storage manifests the largest marginal cost, thus the EDN would rather adopt electricity from upstream power grid than hydrogen storage. However, the former is noticeably costly than the applied HCNG-to-power (by over 20%), wherefore the proposed **Model 1** is more lucrative for growth.

## VI. CONCLUSION

This paper proposes a two-stage robust Nash bargaining-based benefit sharing mechanism to facilitate stable cooperation between HCNG network and electric distribution network, that are bridged with SOFCs. To effectuate the latent social welfare implied in the efficient energy conversion of HCNG-enabled SOFCs, a stable cooperation framework is firstly proposed based on Nash bargaining. Then, a robust Nash bargaining that incorporates li-ion batteries is proposed to de-risk the EDN's profit collapse from transaction bias. We finally design a two-stage solving strategy to master the proposed model, where the first stage ensures privacy of the two utilities via ADMM, the second stage efficiently dispatches li-ion batteries to withstand the worst operational cases of EDN via emerging BCD algorithm, and the two stages are looped upon C&CG. Numerical study shows that the proposed scheme circumvents profit collapse, fulfills stable gains for both HCNG network and EDN, and reaches a stable social welfare of nearly 1.6% to total cost.

## REFERENCES

- [1] International Renewable Energy Agency, "Global energy transformation: A roadmap to 2050," Abu Dhabi, UAE, 2019, Accessed: Jun. 17, 2021. [Online]. Available: <https://www.irena.org/publications>.
- [2] M. Fan, K. Sun, D. Lane, W. Gu, Z. Li, and F. Zhang, "A Novel Generation Rescheduling Algorithm to Improve Power System Reliability With High Renewable Energy Penetration," *IEEE Trans. Power Syst.*, vol. 33, no. 3, pp. 3349–3357, May 2018.
- [3] J. Duan, F. Liu, and Y. Yang, "Optimal operation for integrated electricity and natural gas systems considering demand response uncertainties," *Applied Energy*, vol. 323, p. 119455, Oct. 2022.
- [4] C. He, L. Wu, T. Liu, and M. Shahidehpour, "Robust Co-Optimization Scheduling of Electricity and Natural Gas Systems via ADMM," *IEEE Trans. Sustain. Energy*, vol. 8, no. 2, pp. 658–670, Apr. 2017.
- [5] J. Duan, Y. Yang, and F. Liu, "Distributed optimization of integrated electricity-natural gas distribution networks considering wind power uncertainties," *Int. J. Electr. Power Energy Syst.*, vol. 135, p. 107460, Feb. 2022.
- [6] C. Fu, J. Lin, Y. Song, J. Li, and J. Song, "Optimal Operation of an Integrated Energy System Incorporated With HCNG Distribution Networks," *IEEE Trans. Sustain. Energy*, vol. 11, no. 4, pp. 2141–2151, Oct. 2020.
- [7] H. Chen, C. Yang, N. Zhou, N. Farida Harun, D. Oryshchyn, and D. Tucker, "High efficiencies with low fuel utilization and thermally integrated fuel reforming in a hybrid solid oxide fuel cell gas turbine system," *Applied Energy*, vol. 272, p. 115160, Aug. 2020.
- [8] A. S. Mehr, A. Moharramian, S. Hossainpour, and D. A. Pavlov, "Effect of blending hydrogen to biogas fuel driven from anaerobic digestion of wastewater on the performance of a solid oxide fuel cell system," *Energy*, vol. 202, p. 117668, Jul. 2020.
- [9] Q. Hou, H. Zhao, and X. Yang, "Economic performance study of the integrated MR-SOFC-CCHP system," *Energy*, vol. 166, pp. 236–245, Jan. 2019.
- [10] A. Nikoobakht, J. Aghaei, M. Shafie-Khah, and J. P. S. Catalao, "Continuous-Time Co-Operation of Integrated Electricity and Natural Gas Systems With Responsive Demands Under Wind Power Generation Uncertainty," *IEEE Trans. Smart Grid*, vol. 11, no. 4, pp. 3156–3170, Jul. 2020.
- [11] H. K. Nguyen, A. Khodaei, and Z. Han, "Incentive Mechanism Design for Integrated Microgrids in Peak Ramp Minimization Problem," *IEEE Trans. Smart Grid*, vol. 9, no. 6, pp. 5774–5785, Nov. 2018.
- [12] N. Valitov, "Risk premia in the German day-ahead electricity market revisited: The impact of negative prices," *Energy Economics*, vol. 82, pp. 70–77, Aug. 2021.
- [13] A. Jiang, H. Yuan, and D. Li, "Energy management for a community-level integrated energy system with photovoltaic prosumers based on bargaining theory," *Energy*, vol. 225, Jun. 2021.
- [14] S. Fan, Q. Ai, and L. Piao, "Bargaining-based cooperative energy trading for distribution company and demand response," *Appl. Energy*, vol. 226, pp. 469–482, Sep. 2018.
- [15] R.-P. Liu, Y. Hou, Y. Li, S. Lei, W. Wei, and X. Wang, "Sample Robust Scheduling of Electricity-Gas Systems Under Wind Power Uncertainty," *IEEE Trans. Power Syst.*, vol. 36, no. 6, pp. 5889–5900, Nov. 2021.
- [16] J. Snoussi, S. B. Elghali, M. Benbouzid, and M. F. Mimouni, "Optimal Sizing of Energy Storage Systems Using Frequency-Separation-Based Energy Management for Fuel Cell Hybrid Electric Vehicles," *IEEE Trans. Veh. Technol.*, vol. 67, no. 10, pp. 9337–9346, Oct. 2018.
- [17] Q. Li, Y. Qiu, H. Yang, Y. Xu, W. Chen, and P. Wang, "Stability-constrained two-stage robust optimization for integrated hydrogen hybrid energy system," *CSEE JPES*, 2020.
- [18] G. Qin, Q. Yan, D. Kammen, C. Shi, and C. Xu, "Robust optimal dispatching of integrated electricity and gas system considering refined power-to-gas model under the dual carbon target," *J. Clean. Prod.*, vol. 371, Oct. 2022.
- [19] J. Lu, T. Liu, C. He, L. Nan, and X. Hu, "Robust day-ahead coordinated scheduling of multi-energy systems with integrated heat-electricity demand response and high penetration of renewable energy," *Renew. Energy*, vol. 178, pp. 466–482, Nov. 2021.
- [20] B. Bagheri and N. Amjadi, "Adaptive-robust multi-resolution generation maintenance scheduling with probabilistic reliability constraint," *IET Gener. Transm. Distrib.*, vol. 13, no. 15, pp. 3292–3301, Aug. 2019.
- [21] M. Abeysekera, J. Wu, N. Jenkins, and M. Rees, "Steady state analysis of gas networks with distributed injection of alternative gas," *Appl. Energy*, vol. 164, pp. 991–1002, Feb. 2016.
- [22] F. Liu, Z. Bie, and X. Wang, "Day-Ahead Dispatch of Integrated Electricity and Natural Gas System Considering Reserve Scheduling and Renewable Uncertainties," *IEEE Trans. Sustain. Energy*, vol. 10, no. 2, pp. 646–658, Apr. 2019.
- [23] L. Yang, X. Zhao, and Y. Xu, "A convex optimization and iterative solution based method for optimal power-gas flow considering power and gas losses," *Int. J. Electr. Power Energy Syst.*, vol. 121, p. 106023, Oct. 2020.
- [24] M. Chen, Z. Liang, Z. Cheng, J. Zhao, and Z. Tian, "Optimal Scheduling of FTPSS With PV and HESS Considering the Online Degradation of Battery Capacity," *IEEE Trans. Transp. Electrific.*, vol. 8, no. 1, pp. 936–947, Mar. 2022.
- [25] F. Dababneh and L. Li, "Integrated Electricity and Natural Gas Demand Response for Manufacturers in the Smart Grid," *IEEE Trans. Smart Grid*, vol. 10, no. 4, pp. 4164–4174, Jul. 2019.



> REPLACE THIS LINE WITH YOUR MANUSCRIPT ID NUMBER (DOUBLE-CLICK HERE TO EDIT) <

- [26]V. Khaligh, A. Ghezelbash, M. Mazidi, J. Liu, and J.-H. Ryu, "P-robust energy management of a multi-energy microgrid enabled with energy conversions under various uncertainties," *Energy*, vol. 271, p. 127084, May 2023.
- [27]N. Tomin, V. Kurbatsky, K. Suslov, D. Gerasimov, E. Serdyukova, and D. Yang, "Flexibility-based improved energy hub model for multi-energy distribution systems," IET Conference Proceedings, vol. 2022, no. 3. IET, UK, pp. 409–13, 2022.
- [28]A. Ehsan and Q. Yang, "Coordinated Investment Planning of Distributed Multi-Type Stochastic Generation and Battery Storage in Active Distribution Networks," *IEEE Trans. Sustain. Energy*, vol. 10, no. 4, pp. 1813–1822, Oct. 2019.